

Fluid Shear Stress-Induced Down-Regulation of miR-146a-5p Inhibits Osteoblast Apoptosis via Targeting SMAD4

Xuening LIU^{1,2#}, Kun ZHANG^{3#}, Lifu WANG^{1,2}, Bin GENG^{1,2}, Zhongcheng LIU^{1,2}, Qiong YI^{1,2}, Yayi XIA^{1,2}

[#]These authors contributed equally to this work

¹Department of Orthopaedics, Lanzhou University Second Hospital, Lanzhou Gansu, China,

²Orthopaedics Key Laboratory of Gansu Province, Lanzhou Gansu, China, ³Department of Orthopaedics, Honghui Hospital, Xi'an Jiaotong University, Xi'an Shaanxi, China

Received May 4, 2021

Accepted September 22, 2022

Epub Ahead of Print October 13, 2022

Summary

Fluid shear stress (FSS) plays an important role in osteoblast apoptosis. However, the role of miRNA in osteoblast apoptosis under FSS and possible molecular mechanisms remain unknown. Our aim of the study was to explore whether miR-146a-5p regulates osteoblast apoptosis under FSS and its molecular mechanisms. FSS could down-regulate the expression of miR-146a-5p in MC3T3-E1 cells. We confirm that up-regulation of miR-146a-5p promotes osteoblasts apoptosis and down-regulation of miR-146a-5p inhibits osteoblasts apoptosis. We further demonstrated that FSS inhibits osteoblast apoptosis by down-regulated miR-146a-5p. Dual-luciferase reporter assay validated that SMAD4 is a direct target gene of miR-146a-5p. In addition, mimic-146a-5p suppressed FSS-induced up-regulation of SMAD4 protein levels, which suggests that FSS elevated SMAD4 protein expression levels via regulation miR-146a-5p. Further investigations showed that SMAD4 could inhibit osteoblast apoptosis. We demonstrated that miR-146a-5p regulates osteoblast apoptosis via targeting SMAD4. Taken together, our present study showed that FSS-induced down-regulation miR-146a-5p inhibits osteoblast apoptosis via target SMAD4. These findings may provide novel mechanisms for FSS to inhibit osteoblast apoptosis, and also may provide a potential therapeutic target for osteoporosis.

Keywords

Fluid shear stress • miR-146a-5p • SMAD4 • Osteoblast apoptosis

Corresponding author

Yayi Xia, Department of Orthopaedics, Lanzhou University Second Hospital, Lanzhou Gansu, 730000, China. E-mail: xiayayilzu@outlook.com

Introduction

Mechanical stimulation plays an important role in modulating cellular responses and regulating bone remodeling and bone homeostasis [1]. The lack of mechanical stimulation owing to aging or exposure to an external mechanical unloading environment (e.g., prolonged bed rest, hindlimb unloading, or under conditions of microgravity) may reduce bone formation, weaken the bone structure, and accelerate the loss of bone quantity and quality, further leading to the development of osteoporosis [2-5]. Fluid shear stress (FSS) was a major mechanical stimulus within bone tissue and plays an important role in the process of bone metabolism, it could promote osteoblast proliferation and inhibits osteoblast apoptosis through activating various signal transduction pathways [6, 7].

MicroRNAs are short-stranded non-coding RNAs, which can regulate gene expression by inhibiting the translational efficiency of mRNAs or leading to mRNA degradation [8]. It plays an important role in various physiological and pathological processes, such as cell differentiation, proliferation, apoptosis, and tumorigenesis [9-11]. MicroRNAs have recently been found to be involved in the process of bone metabolism. Park *et al.* [12] found that miR-23 plays an important role in inhibiting bone formation and maintaining bone homeostasis in mice. Chen *et al.* [13] found that miR-34a inhibits osteoblast differentiation and bone formation.

MiR-146a-5p was a mechanosensitive miRNA

and sensitive to various mechanical stimuli. Troidl *et al.* [14] found that FSS could up-regulate the expression of miR-146a-5p in vascular cells. Iwawaki *et al.* [15] found that the expression level of miR-146a-5p was increased in MC3T3-E1 cells under compressive forces. Recent studies have shown that miR-146a-5p is closely associated with bone formation and osteoblasts [16, 17]. Zheng *et al.* [18] demonstrated that miR-146a-5p is a key repressor in bone formation. They found that mice with miR-146a-5p knockout showed increased bone formation and bone mass in vivo. In addition, they found that the expression of miR-146a-5p in the femurs of female mice and female patients gradually increased with age, and miR-146a-5p deletion could delay age-induced bone loss in female mice. These findings suggest that miR-146a-5p may be a potential target to improve osteoporosis. However, little is known about whether miR-146a-5p has an influence on osteoblast apoptosis under FSS and the underlying mechanism of this effect. Based on the above theory, we propose the hypothesis: of whether FSS affects miR-146a-5p expression level in osteoblasts and further affects osteoblast apoptosis, and how miR-146a-5p regulates osteoblast apoptosis under FSS.

In the present study, we investigated the expression of miR-146a-5p under FSS. We explore the role of miR-146a-5p in osteoblast apoptosis and found that FSS-induce down-regulate miR-146a-5p could inhibit osteoblast apoptosis. Next, we further examine SMAD4 as a direct target gene of miR-146a-5p and found that FSS-induced down-regulation miR-146a-5p inhibits osteoblast apoptosis by targeting SMAD4. The study may provide some new mechanisms for FSS to inhibit osteoblast apoptosis and also may provide a potential target for the treatment of osteoporosis.

Materials and Methods

Cell culture

The mouse osteoblastic MC3T3-E1 cells were obtained from the Chinese Academy of Medical Sciences (Beijing, China). Cells were cultured with α-MEM containing 10 % fetal bovine serum (FBS) and were maintained in a moist environment containing 5 % CO₂ at 37 °C.

FSS experiment

The MC3T3-E1 cells were seeded on 20 × 50 mm coverslips. When cells were close to 90 % confluence, cells were incubated in a serum-free medium

for 6 h before being exposed to FSS at 12 dyn/cm² for 1 h. Cells were exposed to laminar flow in parallel plate flow chambers. This system can provide continuous hydrostatic pressure to drive the medium through the channel of the parallel plate flow chamber to generate a precise FSS. During the FSS experiment, the system was maintained at 37 °C.

Cell transfection

The miRNA regulator (mimic and inhibitor) was purchased from Ribo Biotechnology, China. Cells were seeded on 20 × 50 mm coverslips. When cells were close to 50-75 % confluence and then transfected with miRNA regulators using a transfection reagent (Ribo Biotechnology, China). The transfection concentration of miR-146a-5p mimic and its negative control was 50 nM. The transfection concentration of miR-146a-5p inhibitor and its negative control was 100 nM. GP-transfect-Mate (GenePharma, China) was used for the transfection of siRNA-SMAD4 (GenePharma, China) or pcDNA3.1-SMAD4 (GenePharma, China). siRNAs were transfected at a concentration of 50 nM. Plasmids were transfected at a concentration of 0.5-1.5 ug. MC3T3-E1 cells were transfected for 48 h.

Western blot analysis

After washing twice with PBS, cells were lysed with RIPA buffer (Beyotime Biotechnology, China) containing protease and phosphatase inhibitors supplemented with 1 mmol/LPMSF. Cell debris was removed by centrifugation at 12000 rpm for 20 min at 4 °C after on ice for 20–30 min, and the protein concentration was detected using a BCA protein assay kit (Beyotime Biotechnology, China). A mixture containing cell lysate and 4x protein loading buffer was boiled for 5-10 min. The proteins were separated with 10 or 12 % SDS-PAGE and transferred to PVDF membranes. The membranes were blocked with QuickBlock™ Western blocking buffer (Beyotime Biotechnology, China) for 30 min at room temperature. The membranes were then incubated with primary antibodies including β-actin (1:20000, Proteintech, USA), caspase-3 (1:1000, Cell Signaling Technology, USA), Bax (1:5000, Proteintech, USA), Bcl-2 (1:2000, Proteintech, USA) and SMAD4 (1:1000, Cell Signaling Technology, USA) overnight 4 °C. Next, after washing three times with 1×Tris Buffered Saline with Tween (TBST), the membranes were incubated with horseradish peroxidase (HRP)-conjugated immunoglobulin G (IgG) secondary antibody

(1:1500, ZSGB-BIO, China) for 2 h at room temperature. Finally, the blotted bands were observed using the Super Signal West Pico Chemiluminescent Substrate (Thermo Fisher Scientific Inc., USA) and imaged by a VersaDoc Imaging System (Bio-Rad Laboratories Co., USA). Quantitative analysis of the results was performed using Image-Pro Plus 6.0 software.

RNA extraction and real-time PCR analysis

We carefully extracted total RNA from MC3T3-E1 cells with the TRIzol Reagent (Invitrogen, USA). The concentration and purity of total RNA were detected by measuring absorbance at 260 nm and 280 nm using a NanoDrop ND-1000 Spectrophotometer (Thermo Fisher). For miRNA, the Mir-X miRNA First-Strand Synthesis Kit (TaKaRa, Japan) was used to synthesize cDNA. Then, quantitative real-time PCR was accomplished by using an SYBR Green Pro Taq HS Premix (Accurate biology, China). Small nuclear RNA U6 was selected as an internal reference for miR-146a-5p. For mRNA, Evo M-MLV RT Kit with gDNA Clean for qPCR (Accurate biology, China) was used to synthesize cDNA. The expression levels of mRNA were detected quantitatively by an LC-96 real-time PCR detection system (Roche, USA) using SYBR Green Pro Taq HS Premix (Accurate biology, China) according to the manufacturer's protocols. GAPDH was selected as an internal reference for mRNA. Primer sequences used for qPCR were shown in Table 1. Relative expression levels (fold change) were calculated using the $2^{-\Delta\Delta Ct}$ methods.

Immunofluorescence assay

After rinsing three times with PBS, cells were fixed using 4 % paraformaldehyde for 15 min,

permeabilized with 0.1 % Triton X-100 for 30 min, blocked with 10 % goat serum for 1 h at 37 °C, and incubated with anti-SMAD4 primary antibody (1:100, Proteintech, USA) overnight at 4 °C. Re-warm for 1 h at 37 °C, the cell incubated with Alexa Fluor 488-conjugated secondary antibody (1:300, ProteinTech, USA) for 1 h at 37 °C in the darkroom. All cells were stained with 10 % DAPI for 10-15 min at room temperature in the dark. Cells were observed by immunofluorescence microscopy (Olympus, Japan).

Dual-luciferase assay

293T cells were selected for dual-luciferase experiments due to low endogenous expression. Wild-type (WT) or mutant (MUT) 3' UTR fragments of mouse-derived SMAD4 were provided by Gemma (Shanghai, China). SMAD4 WT or MUT 3'UTR reporter vector and miR-146a-5p (mimic, inhibitor, or their negative controls) were co-transfected into the cells using GP-transfect-Mate (GenePharma, China) as instructed by the manufacturer. Cells were harvested 48 h after transfection. The value of fluorescence detected by the luciferase assay kit (Promega, USA) according to the manufacturer's protocol.

Hoechst 33258 staining

The MC3T3-E1 cells were seeded on 20 × 50 mm coverslips. When cells were close to 75 % confluence, cells were rinsed three times with PBS. After fixation with 4 % paraformaldehyde for 15 min at room temperature, the cell was stained with Hoechst 33258 for 10 min at room temperature in the dark. The nuclear morphological changes were observed by fluorescence microscope (Olympus, Japan) after rinsing three times with PBS.

Table 1. Sequences of the primers for qRT-PCR

Name	Forward (5'-3')	Reverse (5'-3')
Bax	GGATGCGTCCACCAAGAAG	CAAAGTAGAACAGGGCAACCAC
Bcl-2	GATGACTTCTCTCGTCGCTAC	GAACCTCAAAGAAGGCCACAATC
Caspase-3	GAAACTCTTCATCATTCAAGGCC	GCGAGTGAGAATGTGCATAAAAT
SMAD4	AGTTCACAAATGAGCTTCATT	TTCAAAGTAAGCAATGGAGCAC
miR-146a-5p	CGCTGAGAACTGAATTCCATGGGTT	
U6	CTCGCTTCGGCAGCACA	AACGCTTCACGAATTGCGT
GAPDH	TGTGTCCGTCGTGGATCTGA	TTGCTGTTGAAGTCGCAGGAG

TUNEL assay

TdT mediated dUTP nick end labeling (TUNEL) assay was used to further detect apoptotic cells by TUNEL apoptosis detection kit (Yeasen, China) according to the manufacturer's instruction. Firstly, the prepared cells were fixed with 4 % paraformaldehyde for 15 min, permeabilized with 0.1 % Triton X-100 for 30 min, and then incubated with 100 μ l 1 \times equilibration buffer for 30 min at room temperature. Next, the cell was incubated with a TUNEL reaction mixture in a humidified atmosphere for 1 h at 37°C in the dark, then stained with DAPI for 10 min at room temperature after rinsing three times with PBS. Finally, the sample was analyzed by a fluorescent microscope.

Flow cytometry

FITC Annexin V apoptosis detection kit I (BD Biosciences, USA) was used to detect the apoptosis rate of MC3T3-E1 cells. Cells were washed twice with cold PBS and then resuspended in 1 \times binding buffer. Gently vortex the cells and incubate for 15 min at room temperature in the dark after adding 5 μ l of FITC Annexin V and 5 μ l PI. The apoptosis rate was detected by a flow cytometer (BECKMAN CytoFLEX, USA).

Statistical analysis

GraphPad Prism version 8.0 was used as statistical analysis software. All data are presented as the mean \pm SD. All statistical analyses were performed through one-way ANOVA. For the post hoc test, Tukey was used. P -values < 0.05 were considered statistically significant.

Results

Down-regulation of miR-146a-5p in MC3T3-E1 cell under FSS

To explore whether the expression of miR-146a-5p in MC3T3-E1 cells was affected by FSS, MC3T3-E1 cells were exposed to FSS (12 dyn/cm²) for 0, 30, 60, 90, and 120 min. Then, total RNA was extracted from cells, and the expression level of miR-146a-5p was detected by the qRT-PCR assay. The results (Fig. 1) showed that the expression level of miR-146a-5p in MC3T3-E1 cells was significantly down-regulated in response to FSS, and the expression level was the lowest for 60 min.

miR-146a-5p promotes apoptosis of MC3T3-E1 cells

To investigate the biological effect of miR-146a-5p on osteoblast apoptosis, we up-regulate and down-

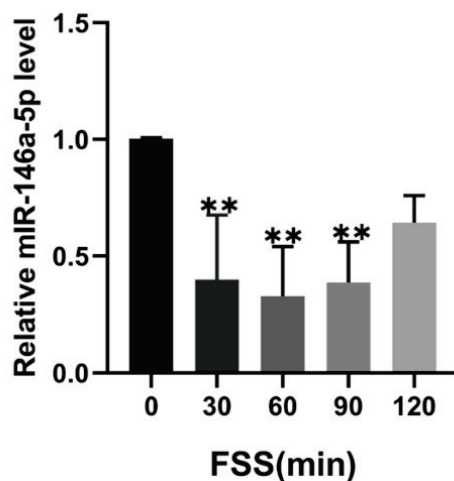


Fig. 1. The expression level of miR-146a-5p in MC3T3-E1 cells was downregulated in response to FSS. The expression level of miR-146a-5p in MC3T3-E1 cells was examined by qRT-PCR after being exposed to FSS (12 dyn/cm²) for 0 (control), 30, 60, 90, and 120 min. The data were expressed as mean \pm SD of three independent experiments. ** $p < 0.01$ vs control.

regulate the expression of miR-146a-5p in MC3T3-E1 cells by 146a-5p-mimic and 146a-5p-inhibitor, respectively. The protein expressions of genes associated with cell apoptosis were assessed by western blot. The results showed that the expression levels of Bax and Cleaved Caspase-3 significantly increased following transfection with mimic-146a-5p and decreased markedly following transfection with inhibitor-146a-5p compared with the transfection of mimic-NC or inhibitor-NC, the expression level of Bcl-2 protein was significantly reduced after transfection with mimic-146a-5p and increased after transfection with inhibitor-146a-5p compared with the transfection of mimic-NC or inhibitor-NC (Fig. 2A-D). In addition, the effect of miR-146a-5p on osteoblast apoptosis was further validated by observing cell morphological changes using TUNEL assay and Hoechst 33258 staining. TUNEL assay results showed that the number of TUNEL-positive cells was increased in the mimic-146a-5p group compared with that in the mimic-NC group, while the number of TUNEL-positive cells was decreased in the inhibitor-146a-5p group compared with that in the inhibitor-NC group (Fig. 2E,F). The same result was observed in Hoechst 33258 staining (Fig. 2G,H). These results suggested that miR-146-5p is a promoter of osteoblast apoptosis.

Up-regulation of miR-146a-5p partially attenuates the effect of FSS to inhibit osteoblast apoptosis

Our previous studies have suggested that FSS could inhibit osteoblast apoptosis [7, 19]. To explore

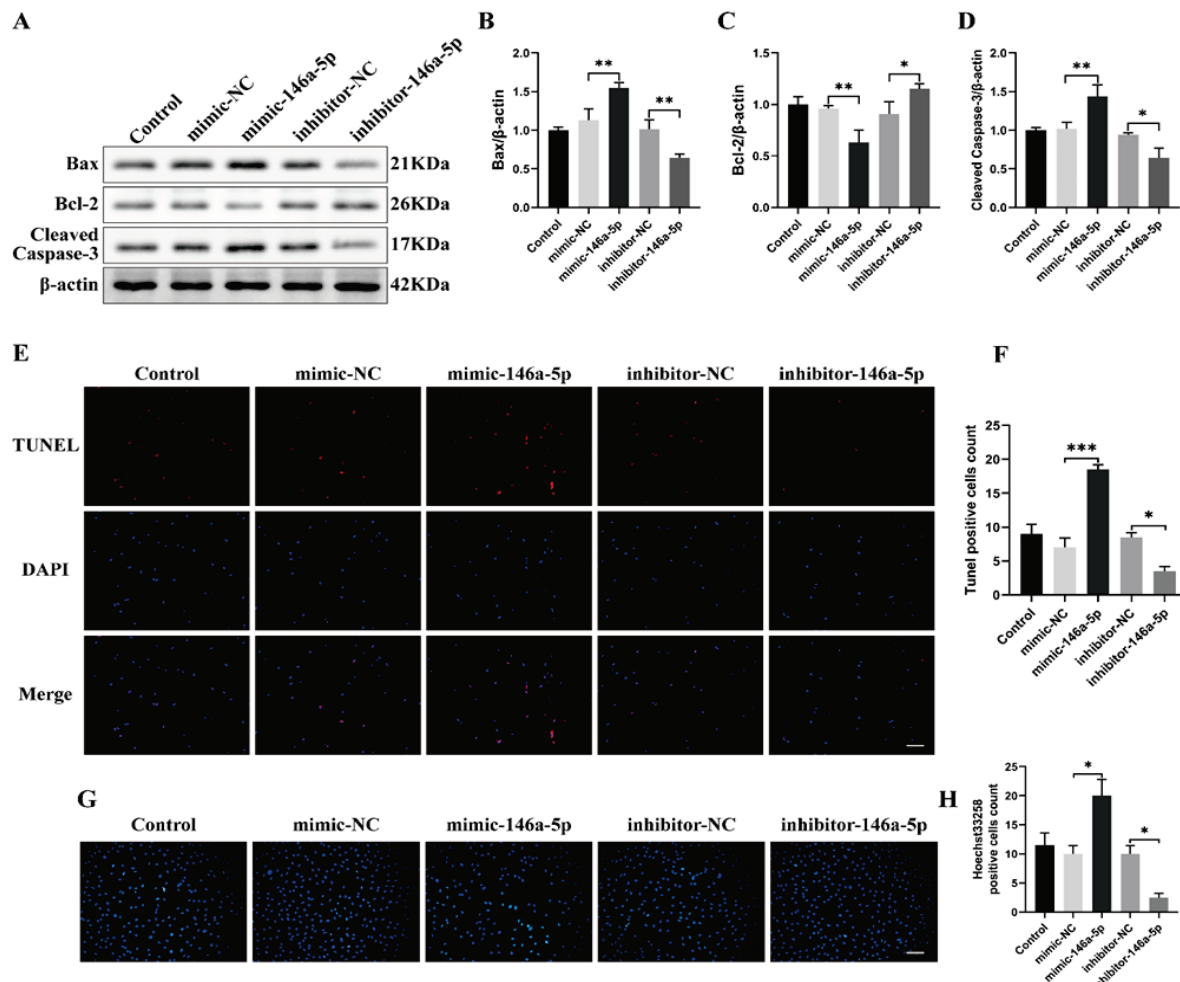


Fig. 2. miR-146a-5p promotes apoptosis of MC3T3-E1 cells. The protein expression level of Bax, Bcl-2, and Cleaved Caspase-3 were examined by western blot (**A**). The ratios of Bax/β-actin, Bcl-2/β-actin, and Cleaved Caspase-3/β-actin in different groups were quantified (**B-D**). Apoptotic cells are labeled with TUNEL. Staining of cells with DAPI (blue) and TUNEL (red), respectively. Scale bar = 50 μm (**E**). The percentage of TUNEL-positive cells was statistically analyzed in each group (**F**). Hoechst 33258 staining analysis MC3T3-E1 cells apoptosis, scale bar = 50 μm (**G**). The percentage of Hoechst-positive cells was statistically analyzed in each group (**H**). The data were expressed as mean ± SD of three independent experiments. * $p < 0.05$, ** $p < 0.01$, *** $p < 0.001$.

whether miR-146a-5p is involved in osteoblast apoptosis regulated by FSS, MC3T3-E1 cells were exposed to FSS for 1h after being transfected with mimic-146-5p and its negative control. The results of the qRT-PCR assay and western blot demonstrated that FSS significantly down-regulated the mRNA levels and protein levels of Bax and Caspase-3, and up-regulated the mRNA levels and protein levels of Bcl-2 compared with the control group. In addition, overexpression of miR-146a-5p can markedly weak the decreases of Bax and Caspase-3 levels and the increases of Bcl-2 levels induced by FSS (Fig. 3). These results suggested that up-regulation of miR-146a-5p inhibits the anti-apoptotic effect of FSS.

SMAD4 is a target gene of miR-146a-5p

To obtain more information about the molecular mechanisms by which miR-146a-5p regulates osteoblast

apoptosis. Target genes for miRNA were predicted using three web-based programs: miRDB, miRWALK, and Target Scan. Among these candidate genes, we noticed SMAD4 mRNA, because it is known to be involved in osteoblast apoptosis [20, 21]. We performed dual-luciferase reporters containing either the wild-type SMAD4 3'UTR sequence (WT) or a SMAD4 3'UTR mutant sequence (MUT) of the miR-146a-5p binding site to determine whether miR-146a-5p directly regulates SMAD4 (Fig. 4A). The binding sites for miR-146a-5p were located in the 3' UTR 356-363 sequence of the SMAD4 gene (Fig. 4B). We found that mimic-146a-5p significantly decreased the luciferase reporter activity of SMAD4 3'UTR WT compared to the mimic-146a-5p negative control (mimic-NC), but not SMAD4 3'UTRMUT reporter activity (Fig. 4C). These results demonstrate that SMAD4 is a direct target gene of miR-

146a-5p. We performed western blot and qRT-PCR analysis to further identified the interaction between miR-146a-5p and SMAD4, the results showed that protein and mRNA levels of SMAD4 are influenced by miR-146a-5p (Fig. 4D-F). Immunofluorescence assays suggested that mimic-146a-5p decreased and inhibitor-146a-5p increased the fluorescence activity of SMAD4 (Fig. 4G).

Up-regulation of miR-146a-5p decreases the protein level of SMAD4 induced by FSS

To examine the effect of FSS on expression levels of SMAD4, the MC3T3-E1 cells were exposed to FSS for 1h after transfected mimic-146a-5p and mimic-NC. The mRNA and protein expression levels of SMAD4 were detected by western blot and qRT-PCR analysis. The results showed that FSS increased the mRNA and protein expression levels of SMAD4 compared to the control group. Furthermore, mimic-146a-5p could weaken the up-regulation of mRNA and protein levels of SMAD4 induced by FSS (Fig. 5A-C). The same trend was also shown in immunofluorescence assays (Fig. 5D).

SMAD4 suppresses osteoblast apoptosis

To investigate the role of SMAD4 in osteoblast apoptosis, we overexpressed SMAD4 with an overexpression vector (pcDNA3.1-SMAD4) and knocked down SMAD4 with RNA interference (siRNA-SMAD4) in MC3T3-E1 cells. Western blotting revealed that SMAD4 up-regulation decreased the protein levels of Bax and Cleaved Caspase-3 but increased the protein level of Bcl-2. On the contrary, SMAD4 down-regulation elevated the protein levels of Bax and Cleaved Caspase-3 but reduced the protein levels of Bcl-2. On the contrary, SMAD4 down-regulation elevated the protein levels of Bax and Cleaved Caspase-3 but reduced the protein levels of Bcl-2 (Fig. 6A-D). Moreover, Hoechst 33258 staining suggested that overexpression of SMAD4 inhibited osteoblast apoptosis, whereas knockdown of SMAD4 facilitated osteoblast apoptosis (Fig. 6E,F). The follow-up flow cytometric analysis further demonstrates that the apoptosis rate was significantly down-regulation in pcDNA3.1-SMAD4 transfected cells compared with negative control, while the apoptosis rate was observably up-regulation in siRNA-SMAD4 transfected cells compared with negative control (Fig. 6G,H). These results suggest that SMAD4 plays a role of inhibit osteoblast apoptosis.

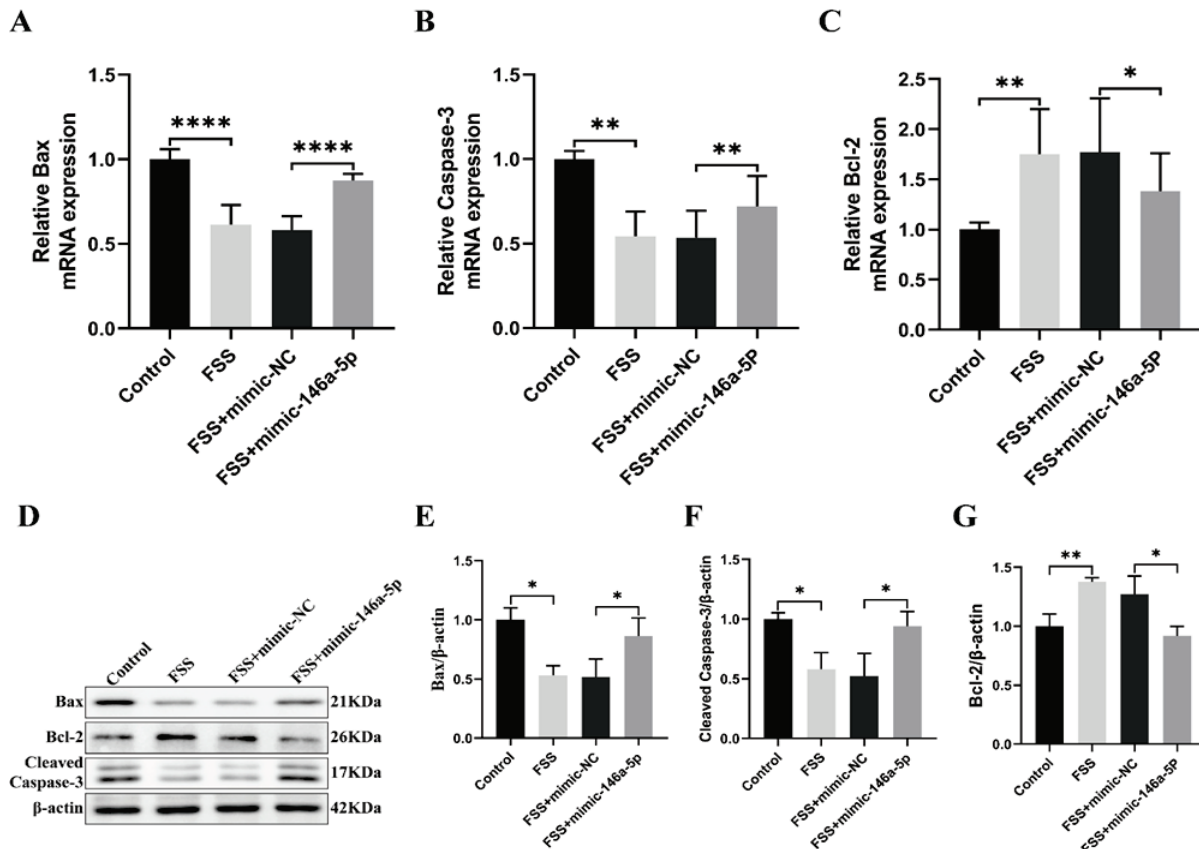


Fig. 3. Up-regulation of miR-146a-5p partially attenuates the effect of FSS to inhibit osteoblast apoptosis. qRT-PCR analysis of the mRNA expression levels of Bax, Caspase-3, and Bcl-2 (**A-C**). The protein expression level of Bax, Bcl-2, and Cleaved caspase-3 were examined by western blot (**D**). The ratios of Bax/β-actin, Bcl-2/β-actin, and Cleaved caspase-3/β-actin in different groups were quantified (**E-G**). The data were expressed as mean ± SD of three independent experiments. * $p<0.05$, ** $p<0.01$, **** $p<0.0001$.

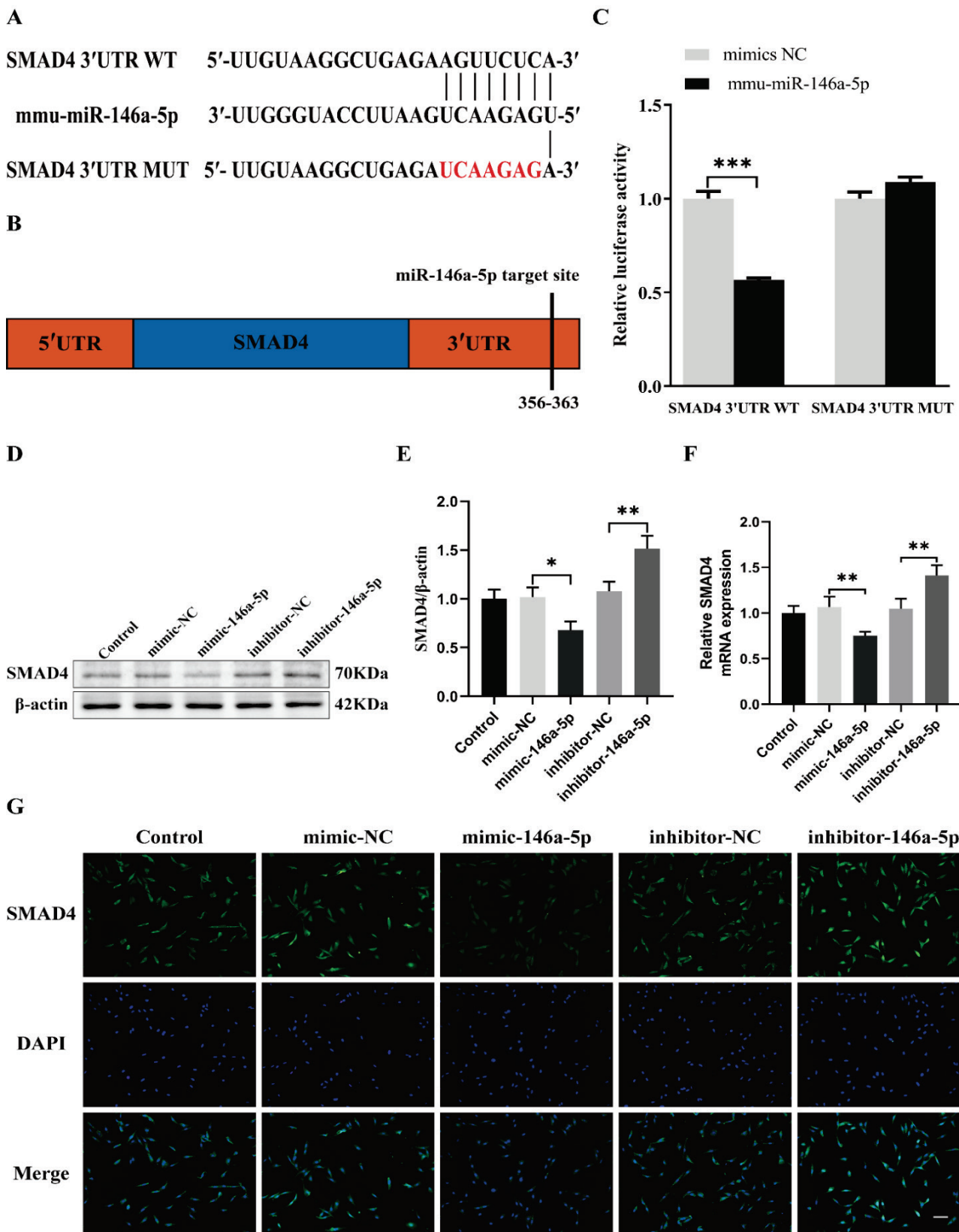


Fig. 4. SMAD4 is a target gene of miR-146a-5p. A schematic illustration of the design of luciferase reporters containing the SMAD4 3'UTR WT or SMAD4 3'UTR MUT (**A**). The predicted SMAD4 binding sites in miR-146a-5p (**B**). The interaction between miR-146a-5p and SMAD4 is identified by luciferase reporter assay (**C**). The protein level of SMAD4 was examined by western blot (**D**). The ratios of SMAD4/β-actin in different groups were quantified (**E**). qRT-PCR analysis of the mRNA expression levels of SMAD4 (**F**). Immunostaining analysis of the SMAD4 protein expression in each group, scale bar = 50 μ m (**G**). The data were expressed as mean \pm SD of three independent experiments. * $p < 0.05$, ** $p < 0.01$, *** $p < 0.001$.

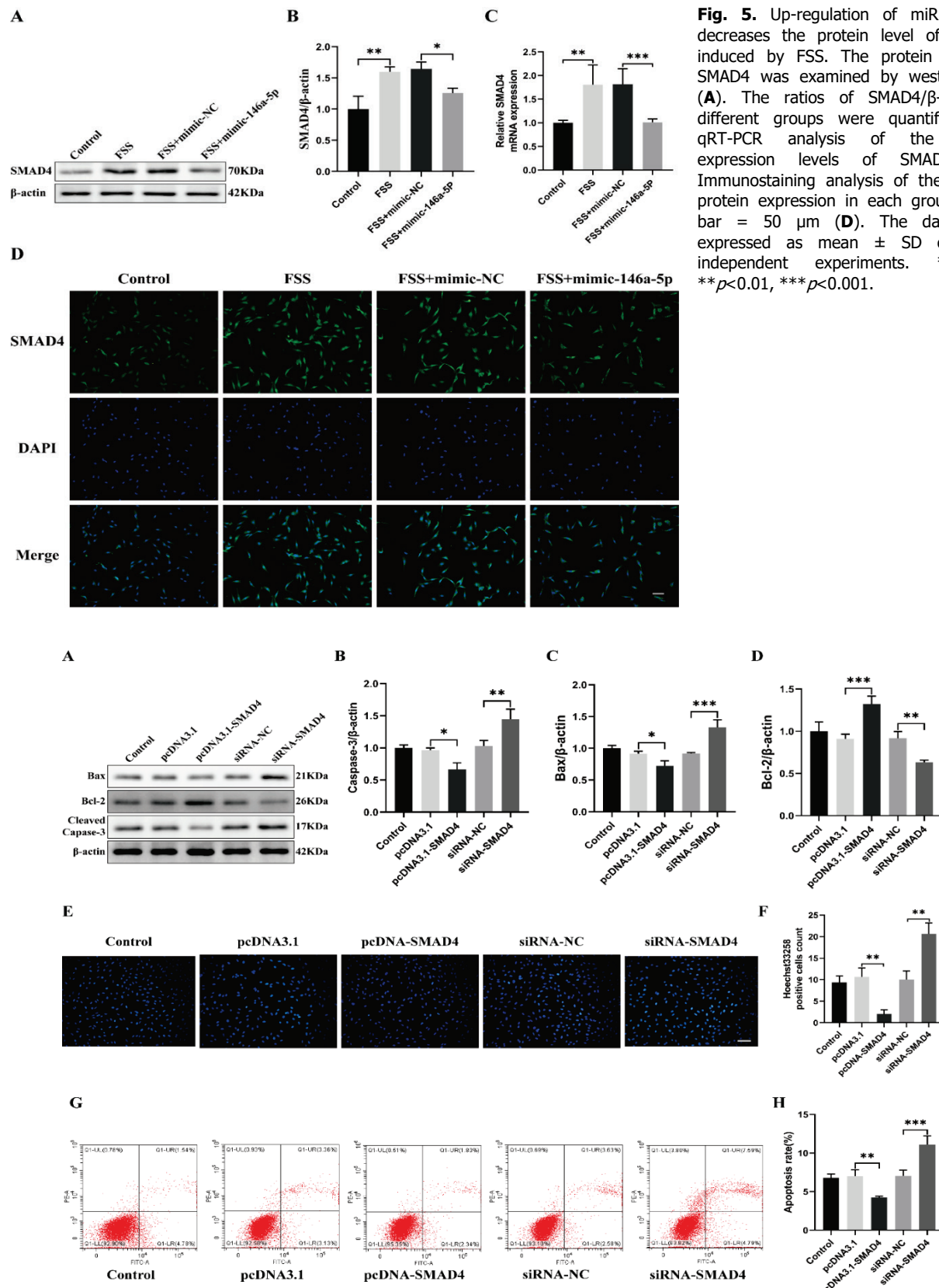


Fig. 5. Up-regulation of miR-146a-5p decreases the protein level of SMAD4 induced by FSS. The protein level of SMAD4 was examined by western blot (**A**). The ratios of SMAD4/β-actin in different groups were quantified (**B**). qRT-PCR analysis of the mRNA expression levels of SMAD4 (**C**). Immunostaining analysis of the SMAD4 protein expression in each group, scale bar = 50 μm (**D**). The data were expressed as mean ± SD of three independent experiments. * $p<0.05$, ** $p<0.01$, *** $p<0.001$.

Fig. 6. SMAD4 suppresses osteoblast apoptosis. The protein level of Bax, Bcl-2, and Cleaved caspase-3 were examined by western blot (**A**). The ratios of Cleaved caspase-3/β-actin, Bax/β-actin, and Bcl-2/β-actin in different groups were quantified (**B-D**). Hoechst 33258 staining analysis MC3T3-E1 cells apoptosis, scale bar = 50 μm (**E**). The percentage of Hoechst-positive cells was statistically analyzed in each group (**F**). The apoptosis rates of MC3T3-E1 cells were evaluated by flow cytometry (**G**). The apoptosis rates were statistically analyzed in each group (**H**). The data were expressed as mean ± SD of three independent experiments. * $p<0.05$, ** $p<0.01$, *** $p<0.001$.

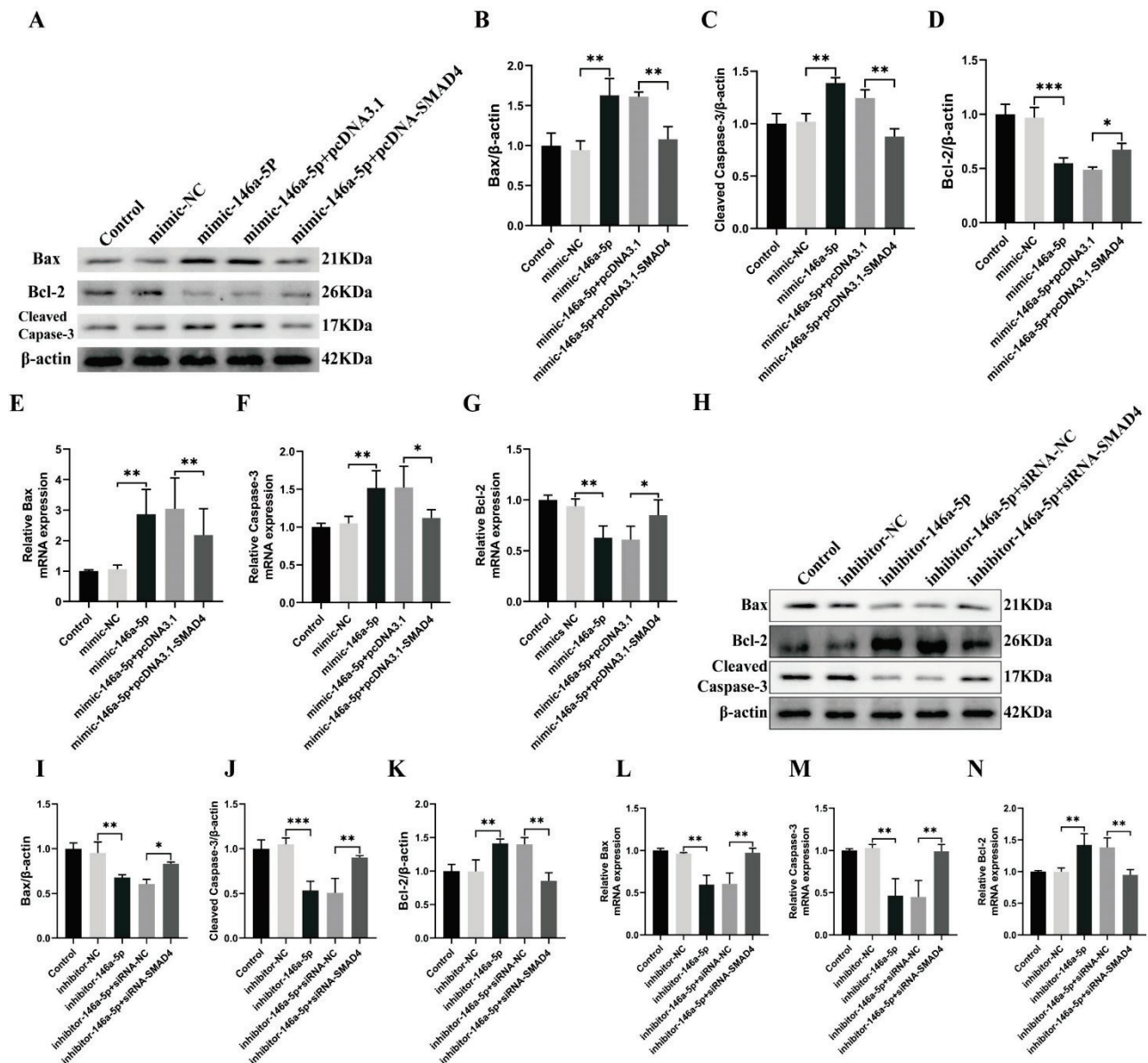


Fig. 7. SMAD4 mediates miR-146a-5p regulated osteoblast apoptosis. The protein level of Bax, Bcl-2, and Cleaved caspase-3 were examined by western blot after the co-transfection of mimic-146a-5p and pcDNA3.1-SMAD4 or their negative controls (**A**). The ratios of Bax/β-actin, Cleaved caspase-3/β-actin, and Bcl-2/β-actin in different groups were quantified (**B-D**). qRT-PCR analysis of the mRNA expression levels of Bax, caspase-3, and Bcl-2 after the co-transfection of mimic-146a-5p and pcDNA3.1-SMAD4 or their negative controls (**E-G**). The protein level of Bax, Bcl-2 and Cleaved caspase-3 were examined by western blot after the co-transfection of inhibitor-146a-5p and siRNA-SMAD4 or their negative controls (**H**). The ratios of Bax/β-actin, Cleaved caspase-3/β-actin, and Bcl-2/β-actin in different groups were quantified (**I-K**). qRT-PCR analysis of the mRNA expression levels of Bax, caspase-3, and Bcl-2 after the co-transfection of inhibitor-146a-5p and siRNA-SMAD4 or their negative controls (**L-N**). The data were expressed as mean ± SD of three independent experiments. * $p<0.05$, ** $p<0.01$, *** $p<0.001$.

SMAD4 mediates miR-146a-5p regulated osteoblast apoptosis

To further confirm whether SMAD4 is involved in osteoblast apoptosis by miR-146a-5p, we co-transfected 146a-5p-mimic with pcDNA3.1-SMAD4 and 146a-5p-inhibitor with siRNA-SMAD4 into MC3T3-E1 cells, respectively. Western blot and qRT-PCR analysis were used to detect the protein and mRNA expression levels of the apoptosis gene. The results showed that

pcDNA3.1-SMAD4 significantly reversed the increased Bax and Cleaved Caspase-3 and decreased Bcl-2 induced by up-regulation of miR-146a-5p (Figure 7 (A-G)), while siRNA-SMAD4 remarkably blocked the decreased Bax and Cleaved caspase-3 and increased Bcl-2 induced by down-regulation of miR-146a-5p (Figure 7 (H-N)). These results suggested that miR-146a-5p promotes apoptosis via regulating SMAD4 in MC3T3-E1 cells.

Discussion

As a common physiological stress stimulation in bone, FSS plays an important role in bone metabolism. Numerous studies showed that many molecules and signaling pathways are involved in FSS-induced proliferation, apoptosis, and differentiation. FSS induces osteoblasts proliferation and differentiation through NOS/NO and COX/PGI2/PGE2 signaling pathways [22]. Our laboratory found that FSS promotes the proliferation of osteoblasts via activation of ERK-5 [23-25], and inhibits the apoptosis of osteoblasts via the ERK5-AKT-FoxO3a-Bim/FasL pathway [19]. Recent studies revealed that many miRNAs are involved in bone metabolic processes under the induction of FSS. Wang *et al.* [26] found that miR-33-5p is involved in FSS-induced osteoblast differentiation. Qi *et al.* [27] reported that miR-132 plays an important role in the differentiation and proliferation of periodontal ligament cells induced by FSS. Our laboratory found that FSS promotes osteoblast proliferation and inhibits osteoblast apoptosis through miRNAs [6,7,28]. Although many studies have identified the molecular mechanism by which FSS inhibits osteoblast apoptosis, the role of miR-146a-5p in FSS-induced inhibition of osteoblast apoptosis remains unknown. In this study, we found that FSS could inhibit the apoptosis of osteoblasts by down-regulate the expression level of miR-146a-5p.

As a non-coding RNA, miR-146a-5p is involved in the regulatory process of metabolism in various tissues. miR-146a-5p is involved in the development of various tumors, including esophageal cancer [29], ovarian cancer [30], pancreatic cancer [31], prostate cancer [32], breast cancer [33], and gastric cancer [34]. In addition, as mentioned earlier in the introduction, miR-146a-5p has been verified as an indispensable regulator of osteoblast apoptosis and bone formation. The present study extends these early findings. Our study results showed that up-regulation of miR-146a-5p could promote osteoblast apoptosis and down-regulation of miR-146a-5p inhibit osteoblast apoptosis. Furthermore, up-regulation of miR-146a-5p could partially attenuate the effect of FSS inhibiting osteoblast apoptosis. These results indicated that miR-146a-5p was involved in the process of FSS inhibiting osteoblast apoptosis.

Studies have shown that miRNAs function mainly by regulating the expression of target genes. Hu *et al.* [35] reported that miR-146a promoted cervical cancer cell viability by targeting IRAK1 and TRAF6.

Chen *et al.* [36] found that miR-146a promoted the apoptosis of gastric cancer cells by targeting TAK1. Shi *et al.* [37] demonstrated that miR-146a increased the sensitivity of cell lung cancer to chemotherapeutic drugs through downregulating CCNJ. Gao *et al.* [38] found that miR-146a regulates the proliferation of breast cell carcinoma through the target gene BRCA1. Crucially, SMAD4 was also shown to be a target gene of miR-146a-5p. Karthikeyan *et al.* [39] demonstrated that miR-146a-5p inhibits the activity of microglia and affects the progression of gliomas by targeting the SMAD4. Kim *et al.* [40] reported that miR-146a-5p promoted the proliferation of gastric cancer cells by downregulating SMAD4. Pu *et al.* [41] found that miR-146a promoted the migration and invasion of melanoma cells by targeting SMAD4. Qiu *et al.* [42] discovered that miR-146a-5p regulated BeWo cell proliferation and apoptosis by targeting SMAD4. Zhang *et al.* [43] found that miR-146a-5p targeting SMAD4 and TRAF6 inhibits adipogenesis through TGF- β and AKT/mTORC1 signal pathways. In the present study, we demonstrated that SMAD4 is a direct target gene of miR-146a-5p. MiR-146a-5p overexpression inhibited SMAD4 protein expression, whereas miR-146a-5p inhibition promoted SMAD4 protein expression, which indicated that miR-146a-5p promotes osteoblast apoptosis through negatively regulated expression of SMAD4 at the post-transcriptional level.

SMAD4, as a member of the SMAD family, is a common mediator in various types of signaling transduction processes of the TGF- β family. SMAD4 is involved in various cellular processes mainly by binding to phosphorylated SMAD to form a complex and then entering the nucleus to regulate the transcription and expression of genes. SMAD4 has been found to play a critical role in various tumors. Mutations in the SMAD4 gene are an unfavorable prognostic marker in colorectal cancer, and loss of SMAD4 expression is associated with poor disease-free survival and overall survival [44]. The expression of SMAD4 is increased in hepatocellular carcinoma and is associated with poor prognosis [45]. SMAD4 is also involved in the development of other tumors, including non-small cell lung cancer [46], prostate cancer [47], and breast cancer [48]. Recently, SMAD4 has also been demonstrated to be involved in processes of bone metabolism. Moon *et al.* [20] found that SMAD4 controlled bone homeostasis by significantly increasing the number of osteoblasts and decreasing osteoclast activity in the trabecular and

cortical regions of mouse femurs. Tan *et al.* [49] demonstrate that SMAD4 silencing significantly inhibited the proliferation and function of osteoblasts, furthermore, osteoblast numbers and bone formation rate were remarkably reduced in SMAD4 mutant mice. It has also been confirmed that SMAD4 is involved in osteoblast differentiation under the regulation of miRNAs [50, 51]. Xiu *et al.* [21] found that SMAD4 could significantly inhibit H₂O₂-induced osteoblast apoptosis, which indicated that SMAD4 was able to ameliorate oxidative stress-induced osteoblast injury. In our study, we found that FSS could up-regulate SMAD4 expression, and overexpression of miR-146a-5p could partially decrease FSS-induced up-regulation of SMAD4 expression. We also demonstrated that SMAD4 was able to inhibit osteoblast apoptosis. Additionally, SMAD4 was a downstream regulator of miR-146a-5p and is involved in the mechanism by which miR-146a-5p regulates osteoblast apoptosis.

In conclusion, we found that the expression of miR-146a-5p was down-regulated in MC3T3-E1 cells under FSS, and the down-regulation of miR-146a-5p could inhibit osteoblast apoptosis. Additionally, we also demonstrated that SMAD4 is a direct target gene of miR-146a-5p, and the up-regulation of SMAD4 was able to inhibit osteoblast apoptosis. Depending on our experimental results, we can conclude that FSS-induced miR-146a-5p down-regulation inhibits osteoblast apoptosis through the target gene SMAD4. Our findings

may provide a novel molecular mechanism for the FSS to inhibit osteoblast apoptosis and new ideas for further research on the effects of mechanical stress on osteoblasts, which offers a new potential target for the treatment of osteoporosis.

Conflict of Interest

There is no conflict of interest.

Acknowledgements

This work was supported by The National Natural Science Foundation of China (81874017 · 81960403 and 82060405), National Science Foundation of Gansu Province of China (20JR5RA320), Cuiying Scientific and Technological Innovation Program of Lanzhou University Second Hospital (CY2017-ZD02, CY2021-MS-A07).

Authors' Contributions

Xuening Liu and Yayı Xia conceived and designed the idea for this paper. Kun Zhang and Lifu Wang participated in the design and coordination of the paper. Qiong Yi and Zhongcheng Liu analyzed the data. Xuening Liu drafted the paper. Bin Geng supervised the framework of the article. All authors read and approved the final version of the manuscript. Xuening Liu was the first author of this article. Xuening Liu and Kun Zhang contributed equally to this work.

References

1. Ozcivici E, Luu Y K, Adler B, Qin Y X, Rubin J, Judex S, Rubin C T. Mechanical signals as anabolic agents in bone. *Nature reviews. Rheumatology* 2010; 6: 50-59. <https://doi.org/10.1038/nrrheum.2009.239>
2. Ng A H, Omelon S, Variola F, Allo B, Willett T L, Alman B A and Grynpas M D. Adynamic bone decreases bone toughness during aging by affecting mineral and matrix. *J Bone Mineral Res* 2016; 31: 369-379. <https://doi.org/10.1002/jbmr.2702>
3. Xin M, Yang Y, Zhang D, Wang J, Chen S, Zhou D. Attenuation of hind-limb suspension-induced bone loss by curcumin is associated with reduced oxidative stress and increased vitamin D receptor expression. *Osteop Int* 2015; 26: 2665-2676. <https://doi.org/10.1007/s00198-015-3153-7>
4. Wang H, Wan Y, Tam K F, Ling S, Bai Y, Deng Y, Liu Y, Zhang H, Cheung W H, Qin L, Cheng J C, Leung K S, Li Y. Resistive vibration exercise retards bone loss in weight-bearing skeletons during 60 days bed rest. *Osteoporosis Int* 2012; 23: 2169-2178. <https://doi.org/10.1007/s00198-011-1839-z>
5. Sibonga J D, Spector E R, Johnston S L, Tarver W J. Evaluating Bone Loss in ISS Astronauts. *Aerospace Med Human Performance* 2015; 86: A38-a44. <https://doi.org/10.3357/AMHP.EC06.2015>
6. Wang X, Geng B, Wang H, Wang S, Zhao D, He J, Lu F, An J, Wang C, Xia Y. Fluid shear stress-induced down-regulation of microRNA-140-5p promotes osteoblast proliferation by targeting VEGFA via the ERK5 pathway. *Connective Tissue Res* 2022; 63: 156-168. <https://doi.org/10.1080/03008207.2021.1891228>

7. Wang X, He J, Wang H, Zhao D, Geng B, Wang S, An J, Wang C, Han H and Xia Y. Fluid shear stress regulates osteoblast proliferation and apoptosis via the lncRNA TUG1/miR-34a/FGFR1 axis. *J Cell Mol Med* 2021; 25: 8734-8747. <https://doi.org/10.1111/jcmm.16829>
8. Peng H, Wang J, Li S. MiR-15a-5p accelerated vascular smooth muscle cells viabilities and migratory abilities via targeting Bcl-2. *Physiol Res* 2022; 71: 667-675. <https://doi.org/10.33549/physiolres.934914>
9. Brennecke J, Hipfner D R, Stark A, Russell R B and Cohen S M. bantam encodes a developmentally regulated microRNA that controls cell proliferation and regulates the proapoptotic gene hid in *Drosophila*. *Cell* 2003; 113: 25-36. [https://doi.org/10.1016/S0092-8674\(03\)00231-9](https://doi.org/10.1016/S0092-8674(03)00231-9)
10. Ambros V. The functions of animal microRNAs. *Nature* 2004; 431: 350-355. <https://doi.org/10.1038/nature02871>
11. MacFarlane LA, Murphy PR. MicroRNA: biogenesis, function and role in cancer. *Curr Genom* 2010; 11: 537-561. <https://doi.org/10.2174/138920210793175895>
12. Park J, Wada S, Ushida T, Akimoto T. The microRNA-23a has limited roles in bone formation and homeostasis in vivo. *Physiological research* 2015; 64: 711-719. <https://doi.org/10.33549/physiolres.932901>
13. Chen L, Holmström K, Qiu W, Ditzel N, Shi K, Hokland L, Kassem M. MicroRNA-34a inhibits osteoblast differentiation and in vivo bone formation of human stromal stem cells. *Stem Cells (Dayton, Ohio)* 2014; 32: 902-912. <https://doi.org/10.1002/stem.1615>
14. Troidl K, Hammerschick T, Albaran-Juarez J, Jung G, Schierling W, Tonack S, Krüger M, Matuschke B, Troidl C, Schaper W, Schmitz-Rixen T, Preissner K T and Fischer S. Shear Stress-Induced miR-143-3p in collateral arteries contributes to outward vessel growth by targeting collagen V- α 2. *Arterio, Thromb, Vasc Biol* 2020; 40: e126-e137. <https://doi.org/10.1161/ATVBAHA.120.313316>
15. Iwawaki Y, Mizusawa N, Iwata T, Higaki N, Goto T, Watanabe M, Tomotake Y, Ichikawa T, Yoshimoto K. MiR-494-3p induced by compressive force inhibits cell proliferation in MC3T3-E1 cells. *J Biosci Bioengineer* 2015; 120: 456-462. <https://doi.org/10.1016/j.jbiosc.2015.02.006>
16. Saferding V, Puchner A, Goncalves-Alves E, Hofmann M, Bonelli M, Brunner J S, Sahin E, Niederreiter B, Hayer S, Kiener H P, Einwallner E, Nehmar R, Carapito R, Georgel P, Koenders M I, Boldin M, Schabbauer G, Kurowska-Stolarska M, Steiner G, Smolen J S, Redlich K and Blüml S. MicroRNA-146a governs fibroblast activation and joint pathology in arthritis. *J Autoimmun* 2017; 82: 74-84. <https://doi.org/10.1016/j.jaut.2017.05.006>
17. Saferding V, Hofmann M, Brunner J S, Niederreiter B, Timmen M, Magilnick N, Hayer S, Heller G, Steiner G, Stange R, Boldin M, Schabbauer G, Weigl M, Hackl M, Grillari J, Smolen JS, Blüml S. microRNA-146a controls age-related bone loss. *Aging Cell* 2020; 19: e13244. <https://doi.org/10.1111/acel.13244>
18. Zheng M, Tan J, Liu X, Jin F, Lai R, Wang X. miR-146a-5p targets Sirt1 to regulate bone mass. *Bone Rep* 2021; 14: 101013. <https://doi.org/10.1016/j.bonr.2021.101013>
19. Bin G, Bo Z, Jing W, Jin J, Xiaoyi T, Cong C, Liping A, Jinglin M, Cuifang W, Yonggang C, Yayi X. Fluid shear stress suppresses TNF- α -induced apoptosis in MC3T3-E1 cells: Involvement of ERK5-AKT-FoxO3a-Bim/FasL signaling pathways. *Exp Cell Res* 2016; 343: 208-217. <https://doi.org/10.1016/j.yexcr.2016.03.014>
20. Moon Y J, Yun C Y, Choi H, Ka S O, Kim J R, Park BH, Cho E S. Smad4 controls bone homeostasis through regulation of osteoblast/osteocyte viability. *Exp Mol Med* 2016; 48: e256. <https://doi.org/10.1038/emm.2016.75>
21. Xiu D, Wang Z, Cui L, Jiang J, Yang H, Liu G. Sumoylation of SMAD 4 ameliorates the oxidative stress-induced apoptosis in osteoblasts. *Cytokine* 2018; 102: 173-180. <https://doi.org/10.1016/j.cyto.2017.09.003>
22. Kapur S, Baylink D J and Lau K H. Fluid flow shear stress stimulates human osteoblast proliferation and differentiation through multiple interacting and competing signal transduction pathways. *Bone* 2003; 32: 241-251. [https://doi.org/10.1016/S8756-3282\(02\)00979-1](https://doi.org/10.1016/S8756-3282(02)00979-1)
23. Li P, Ma Y C, Sheng X Y, Dong H T, Han H, Wang J, Xia Y Y. Cyclic fluid shear stress promotes osteoblastic cells proliferation through ERK5 signaling pathway. *Mol Cell Biochem* 2012; 364: 321-327. <https://doi.org/10.1007/s11010-012-1233-y>

24. Ding N, Geng B, Li Z, Yang Q, Yan L, Wan L, Zhang B, Wang C, Xia Y. Fluid shear stress promotes osteoblast proliferation through the NFATc1-ERK5 pathway. Connective Tissue Res 2019; 60: 107-116. <https://doi.org/10.1080/03008207.2018.1459588>
25. Bo Z, Bin G, Jing W, Cuifang W, Liping A, Jinglin M, Jin J, Xiaoyi T, Cong C, Ning D, Yayi X. Fluid shear stress promotes osteoblast proliferation via the Gaq-ERK5 signaling pathway. Connective Tissue Res 2016; 57: 299-306. <https://doi.org/10.1080/03008207.2016.1181063>
26. Wang H, Sun Z, Wang Y, Hu Z, Zhou H, Zhang L, Hong B, Zhang S, Cao X. miR-33-5p, a novel mechano-sensitive microRNA promotes osteoblast differentiation by targeting Hmga2. Sci Rep 2016; 6: 23170. <https://doi.org/10.1038/srep23170>
27. Qi L and Zhang Y. The microRNA 132 regulates fluid shear stress-induced differentiation in periodontal ligament cells through mTOR signaling pathway. Cell Physiol Biochem 2014; 33: 433-445. <https://doi.org/10.1159/000358624>
28. Zhang K, Liu X, Tang Y, Liu Z, Yi Q, Wang L *et al.* Fluid shear stress promotes osteoblast proliferation and suppresses mitochondrial-mediated osteoblast apoptosis through the miR-214-3p-ATF4 Signaling Axis. Physiol Res. 2022;71(4):527-538. <https://doi.org/10.33549/physiolres.934917>
29. Wang C, Guan S, Liu F, Chen X, Han L, Wang D, Nesa E U, Wang X, Bao C, Wang N and Cheng Y. Prognostic and diagnostic potential of miR-146a in oesophageal squamous cell carcinoma. Brit J Cancer 2016; 114: 290-297. <https://doi.org/10.1038/bjc.2015.463>
30. Cui Y, She K, Tian D, Zhang P and Xin X. miR-146a Inhibits Proliferation and Enhances Chemosensitivity in Epithelial Ovarian Cancer via Reduction of SOD2. Oncol Res 2016; 23: 275-282. <https://doi.org/10.3727/096504016X14562725373798>
31. Ali S, Ahmad A, Aboukameel A, Ahmed A, Bao B, Banerjee S, Philip P A and Sarkar F H. Deregulation of miR-146a expression in a mouse model of pancreatic cancer affecting EGFR signaling. Cancer Lett 2014; 351: 134-142. <https://doi.org/10.1016/j.canlet.2014.05.013>
32. Liu R, Yi B, Wei S, Yang W H, Hart K M, Chauhan P, Zhang W, Mao X, Liu X, Liu C G and Wang L. FOXP3-miR-146-NF- κ B axis and therapy for precancerous lesions in prostate. Cancer Res 2015; 75: 1714-1724. <https://doi.org/10.1158/0008-5472.CAN-14-2109>
33. Bhaumik D, Scott G K, Schokrpur S, Patil C K, Campisi J and Benz C C. Expression of microRNA-146 suppresses NF- κ B activity with reduction of metastatic potential in breast cancer cells. Oncogene 2008; 27: 5643-5647. <https://doi.org/10.1038/onc.2008.171>
34. Kogo R, Mimori K, Tanaka F, Komune S and Mori M. Clinical significance of miR-146a in gastric cancer cases. Clinical cancer research 2011; 17: 4277-4284. <https://doi.org/10.1158/1078-0432.CCR-10-2866>
35. Hu Q, Song J, Ding B, Cui Y, Liang J and Han S. miR-146a promotes cervical cancer cell viability via targeting IRAK1 and TRAF6. Oncology reports 2018; 39: 3015-3024. <https://doi.org/10.3892/or.2018.6391>
36. Chen Y, Zhou B, Xu L, Fan H, Xie J, Wang D. MicroRNA-146a promotes gastric cancer cell apoptosis by targeting transforming growth factor β -activated kinase 1. Mol Med Rep 2017; 16: 755-763. <https://doi.org/10.3892/mmr.2017.6640>
37. Shi L, Xu Z, Wu G, Chen X, Huang Y, Wang Y, Jiang W, Ke B. Up-regulation of miR-146a increases the sensitivity of non-small cell lung cancer to DDP by downregulating cyclin J. BMC cancer 2017; 17: 138. <https://doi.org/10.1186/s12885-017-3132-9>
38. Gao W, Hua J, Jia Z, Ding J, Han Z, Dong Y, Lin Q and Yao Y. Expression of miR-146a-5p in breast cancer and its role in proliferation of breast cancer cells. Oncol Lett 2018; 15: 9884-9888.
39. Karthikeyan A, Gupta N, Tang C, Mallilankaraman K, Silambarasan M, Shi M, Lu L, Ang B T, Ling E A and Dheen S T. Microglial SMAD4 regulated by microRNA-146a promotes migration of microglia which support tumor progression in a glioma environment. Oncotarget 2018; 9: 24950-24969. <https://doi.org/10.18632/oncotarget.25116>
40. Kim DH, Chang MS, Yoon CJ, Middeldorp JM, Martinez OM, Byeon SJ, Rha SY, Kim SH, Kim YS, Woo JH. Epstein-Barr virus BARF1-induced NF κ B/miR-146a/SMAD4 alterations in stomach cancer cells. Oncotarget 2016; 7: 82213-82227. <https://doi.org/10.18632/oncotarget.10511>

41. Pu W, Shang Y, Shao Q and Yuan X. miR-146a promotes cell migration and invasion in melanoma by directly targeting SMAD4. *Oncol Lett.* 2018; 15: 7111-7117. <https://doi.org/10.3892/ol.2018.8172>
42. Qiu M, Li T, Wang B, Gong H, Huang T. miR-146a-5p regulated cell proliferation and apoptosis by targeting SMAD3 and SMAD4. *Protein Peptide Lett.* 2020;27(5):411-8. <https://doi.org/10.2174/0929866526666190911142926>
43. Zhang Q, Cai R, Tang G, Zhang W, Pang W. MiR-146a-5p targeting SMAD4 and TRAF6 inhibits adipogenensis through TGF- β and AKT/mTORC1 signal pathways in porcine intramuscular preadipocytes. *J Animal Sci Biotech.* 2021;12(1):12. <https://doi.org/10.1186/s40104-020-00525-3>
44. Kozak MM, von Eyben R, Pai J, Vossler SR, Limaye M, Jayachandran P *et al.* Smad4 inactivation predicts for worse prognosis and response to fluorouracil-based treatment in colorectal cancer. *J Clin Pathol.* 2015;68(5):341-5. <https://doi.org/10.1136/jclinpath-2014-202660>
45. Torbenson M, Marinopoulos S, Dang DT, Choti M, Ashfaq R, Maitra A *et al.* Smad4 overexpression in hepatocellular carcinoma is strongly associated with transforming growth factor beta II receptor immunolabeling. *Human Pathol.* 2002;33(9):871-876. <https://doi.org/10.1053/hupa.2002.128061>
46. Chen H, Wang JW, Liu LX, Yan JD, Ren SH, Li Y *et al.* Expression and significance of transforming growth factor- β receptor type II and DPC4/Smad4 in non-small cell lung cancer. *Exp Therapeutic Med.* 2015;9(1):227-31. <https://doi.org/10.3892/etm.2014.2065>
47. Ding Z, Wu CJ, Chu GC, Xiao Y, Ho D, Zhang J *et al.* SMAD4-dependent barrier constrains prostate cancer growth and metastatic progression. *Nature.* 2011;470(7333):269-273. <https://doi.org/10.1038/nature09677>
48. Chen H, Zhu G, Li Y, Padia RN, Dong Z, Pan ZK *et al.* Extracellular signal-regulated kinase signaling pathway regulates breast cancer cell migration by maintaining slug expression. *Cancer Res.* 2009;69(24):9228-35. <https://doi.org/10.1158/0008-5472.CAN-09-1950>
49. Tan X, Weng T, Zhang J, Wang J, Li W, Wan H *et al.* Smad4 is required for maintaining normal murine postnatal bone homeostasis. *J Cell Sci.* 2007;120(Pt 13):2162-2170. <https://doi.org/10.1242/jcs.03466>
50. Qin XB, Wen K, Wu XX, Yao ZJ. MiR-183 regulates the differentiation of osteoblasts in the development of osteoporosis by targeting Smad4. *Acta histochemica.* 2021;123(7):151786. <https://doi.org/10.1016/j.acthis.2021.151786>
51. Wu M, Wang H, Kong D, Shao J, Song C, Yang T *et al.* miR-452-3p inhibited osteoblast differentiation by targeting Smad4. *Peer J.* 2021;9:e12228. <https://doi.org/10.7717/peerj.122282>